JSMPM

JOURNALS OF SUSTAINABLE MATERIALS PROCESSING AND MANAGEMENT
e-ISSN: 2821-2843

Vol. 6 No. 1 (2026) 1-19
https://publisher.uthm.edu.my/ojs/index.php/jsmpm

Designing Cyanide-Bridged Single Molecule Magnets

Atsuya Uno[1], Aoi Kaieda[1], Daisuke Nakane[1], Humaira Seema[2], Takashiro Akitsu[1]*

[1] *Department of Chemistry, Faculty of Science, Tokyo University of Science, Tokyo 162-8601, JAPAN*
[2] *Institute of Chemical Sciences, University of Peshawar, Peshawar 25120, PAKISTAN*

*Corresponding Author: akitsu2@rs.tus.ac.jp
DOI: https://doi.org/10.30880/jsmpm.2026.06.01.001

Article Info

Received: 9 January 2026
Accepted: 25 March 2026
Available online: 15 May 2026

Keywords

Cyanide-bridged complexes, molecule based magnets, single molecule magnets, Density Functional Theory, magnetic anisotropic parameters

Abstract

Cyanide-bridged metal complexes, which originated from Prussian blue analogues known for their functions as pigments, optical and magnetic materials, and electrode batteries, are representative molecular magnets that can be designed. Research on these molecular magnets has shifted focus from the realization of ferromagnetic superexchange interactions to external field response, multi-physical properties, and, in recent years, single-molecule magnets as nanomagnets. This review collects examples of cyanide-bridged single-molecule magnets. In addition to the accumulation of experimental data, we also discuss the possibility of molecular design and prediction using computational chemistry based on crystal structure data.

1. Introduction to Magnetic Cyanide-Bridged Complexes

Molecular-based magnetic materials, such as cyanide-bridged magnetic assemblies often known as Prussian blue analogs, have gained growing focus in the past two years, due to their potential usage in magnetic-devices [1–2]. A vast range of structural topologies, from discrete polynuclear complexes to one-dimensional (1D), is produced by the cyanide group's capacity to connect different metal ions. Cyanide-bridged magnetic assemblies provide several advantages over traditional magnets, such as their solubility, multifunctionality [3-6]. Among conventional cyanide-bridged magnetic assemblies [7-9], single-chain magnets (SCMs) [10,11] and single-molecule magnets (SMMs) [12], spin-crossover [13], meta-magnetism [14,15], spin-canting [16] and many other intriguing magnetic features have been discovered as a result of significant advancements in this field. Due to their prospective uses in nanometric magnetic devices, SMMs and SCMs stand out among them due to their distinctive delayed magnetic relaxation and molecular-origin magnetic hysteresis properties.

In the last of 1930s, Prandtl and Mohr published the first report on the preparation of lanthanide(Ln)-based $LnFe(CN)_6 \cdot nH_2O$. By employing X-ray diffraction (XRD) methods, Milligan and associates identified the crystal arrangement of Ln-based $LnFe(CN)_6 \cdot 5H_2O$ in the early 1970s. Motivated by interest in molecular magnetism, a lot of studies have been done in the past 10 years on the synthesis and structures of complexes comprising polycyanometalates and Ln(III) metal ions [17]. When theoretical methods for creating organic magnets were devised in the 1980s, the area of molecular magnetism was born [18]. Tuning the molecular topologies and assembly architectures of the resultant complexes is greatly aided by the addition of an organic ligand or ligands to the cyanometallate. Furthermore, the ligands influence the magnetic interaction mechanism by modulating the electronic structure of paramagnetic metal ions and by providing super-exchange pathways that govern the nature and strength of magnetic coupling. This gives researchers a valuable opportunity to control and regulate the complex system's magnetic properties.

So far, several 0D and 1D discrete clusters and coordination polymers (CPs) have been created using polycyanometallates, including the tetracyanometallate, *trans*-dicyano-, *fac*-tricyano-ligands, and *mer*-tricyano-ligands as well as paramagnetic compounds [2,19–21]. A Mn(III) Schiff base compound and a novel *mer*-tricyano-Fe molecular precursor to create four Fe and Mn complexes with cyanide bridges [22]. Inter-chain π–π stack interactions, a one-dimensional coordination polymer, and a cyanide-bridged heterobimetallic dinuclear entity are all present in the complexes. Both theoretical and empirical examinations of the magnetic characteristics revealed that these complexes exhibit diverse magnetic behaviors: some display antiferromagnetic interactions, characterized by a decrease in the $\chi_M T$ product at low temperatures, whereas others show peculiar ferromagnetic coupling, evidenced by a continuous rise in $\chi_M T$ values upon cooling. The findings provide useful knowledge for creating newer-tricyano-containing precursors for coordination chemistry molecular magnetism systems [22]. The trigonal bipyramidal complex $[Tp_2Cu_3Fe_2(Me_3tacn)_3(CN)_6](ClO_4)_4{\cdot}2H_2O$ (hereafter referred to as SMM-34) was reported using a precursor-based synthetic strategy [23]. In this compound, Tp^- represents hydrotris(pyrazolyl)borate and Me_3tacn denotes 1,4,7-trimethyl-1,4,7-triazacyclononane. In a mixed ethanol/acetonitrile solvent, the assembly of $(Bu_4N)[TpFe(CN)_3]$ and the copper precursor synthesized the SMM-34 complex. Consequently, a three $[(Me^3\text{-tacn})Cu]^{2+}$ group in a triangle connects two opposing $[TpFe(CN)_3]$ groups to produce metal-cyanide cores in the trigonal bipyramidal structure of approximately D_{3h} symmetry (Fig. 1) [23].

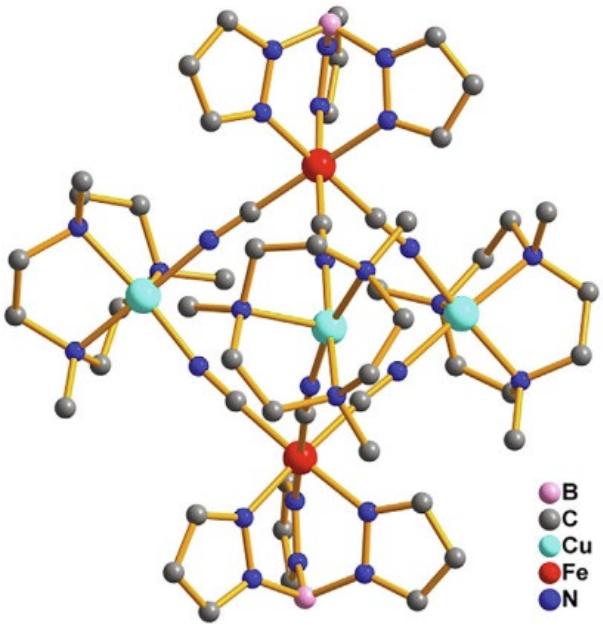

Fig. 1 *Structure of SMM-34 cluster [23]*

When $[Co(III)(CN)_6]^{3-}$ an anionic group reacts with $Co(ClO_4)_2.6H_2O$ according to the alternative blocking ligand results in $[Co(II)(TODA)]\ Co(III)(CN)_6]_2\ 9H_2O$ (hereafter referred to as SMM-72) is obtained [24]. In this structure, TODA represents 1,4,10-Trioxa-7,13-diazacyclopentadecane, a CP with a 2D cyanide-bridges. The XRD research shows that three cyanide units bind the cationic $[Co(II)(TODA)]^{2+}$ groups to the anionic $[Co(III)(CN)6]^{3-}$ results in a 2D honeycomb structure in the crystallographic *bc* plane using a face-coordinated model (Fig. 2 (b)). The somewhat deformed pentagonal bipyramidal configuration of the core Co(II) ion is near the perfect D_{5h} symmetry (Fig. 2 (a)). Meanwhile, direct and alternating current magnetic measurements for the Co(II) complex were acquired. The pentagonal bipyramidal Co(II) ion shows insignificant magnetic interactions by using diamagnetic $[Co(III)(CN)_6]^{3-}$ units, this results in field-inducedSingle-Ion Magnet (SIM) behavior, where $\tau_0 = 3.2 \times 10^{-6}\ s$ and $\Delta/k_B = 12.6\ cm^{-1}$, confirmed by the frequency dependence of the out-of-phase AC susceptibility signals [24].

Cyanide-bridged heterometallic molecular assemblies can be designed using tetracyanometalate building units of the type $[MA(CN)_4(L)]^{n-}$ (n = 1, 2), where L represents a bidentate ligand and M or A corresponds to Fe(II/III) or Cr(III) metal centers coordinated with or without blocking ligands. This strategy allows the formation of a wide variety of architectures, including di-, tri-, tetra-, and hexanuclear complexes, as well as one-, two-, and three-dimensional metal–cyanide frameworks. Among these systems, ferromagnetically coupled 2,4-ribbon-like chains have been reported [19] (Fig. 3). Magnetic measurements indicate that these chains exhibit clear magnetic hysteresis loops at 2.0 K together with frequency-dependent AC susceptibility peaks, suggesting slow magnetic

relaxation behavior. Numerous investigations of such assemblies have therefore produced a wide range of structurally diverse molecular architectures.

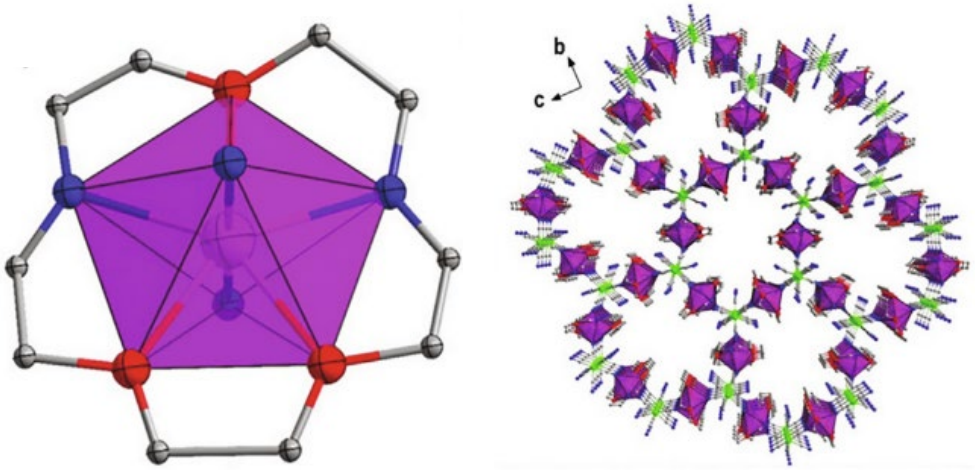

Fig. 2 *(a) In SMM-72, Co(II) ions pentagonal bipyramidal structure; (b) The multilayer 2D honeycomb structure [24]*

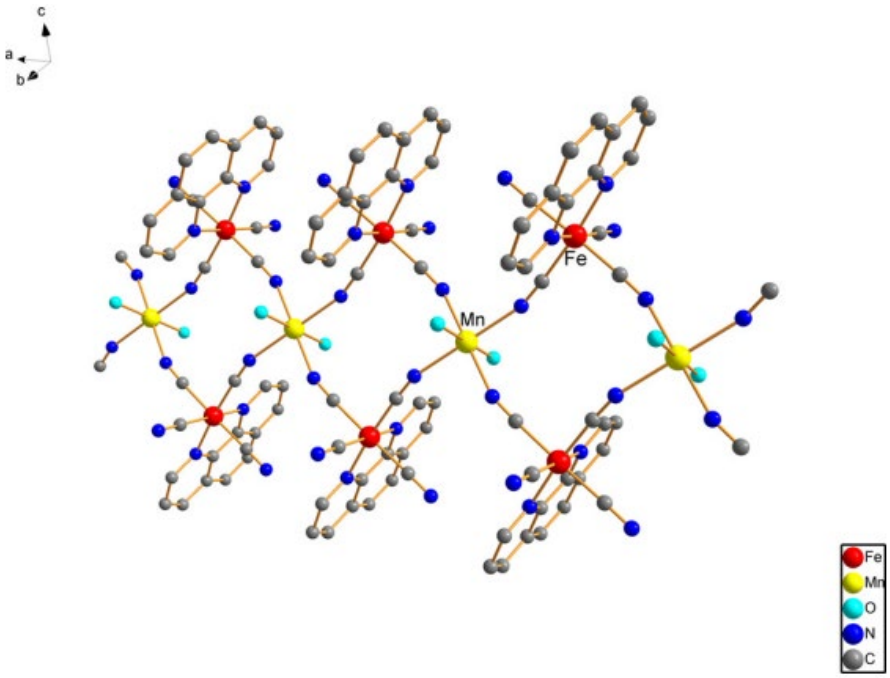

Fig. 3 *Structure of 2,4-ribbon [{Fe(III)2Mn(H2O)(CN)4(phen)}]·4H2O [19]*

2. SMMs and Cyanide-Bridged Compounds

2.1 What is SMM?

Here, we focus on SMMs and delve into their fundamental principles and realization in cyanide-bridged systems. SMM is a material that exhibits magnetic properties with a single molecule. While ordinary magnets are made up of the magnetic interactions of many atoms, SMM is significantly different in that the molecule itself possesses magnetic properties (especially the ability to retain magnetization). There is a lower limit to particle size, determined by the superparamagnetic size, below which magnetization fluctuates freely and information cannot be stored permanently. For magnetic particles with easy axis anisotropy, the magnetization can point in either the "up" or "down" direction. Reorientation of the magnetization occurs by overcoming an anisotropy barrier that is

proportional to the volume of the particle. If the volume is small enough, the magnetization fluctuates freely (superparamagnetic limit) [25]. The single-crystal magnetic susceptibility can be measured parallel or perpendicular to the magnetic axis and magnetic field at low temperature. The resulting hysteresis curves depending on magnetic field sometime indicate clear steps due to tunneling. Highly anisotropic features are fitted using the spin Hamiltonian, which is function of exchange parameter *J*, zero-field-splitting (ZFS) parameters *D* and *E*, and g value. Hamiltonian includes the higher–order terms. For quantitative consideration of relaxation dynamics, magnetization relaxation experiments at fixed magnetic field can be measured, and the relaxation depends on both magnetic field and temperature. Relaxation times τ were obtained from single-exponential fits to the relaxation curves for various magnetic field and temperature conditions. The temperature dependence of τ was fitted with the Arrhenius law $\tau=\tau_0 exp(\Delta E/kT)$ [26]. Furthermore, the basic characteristics of SMMs are expressed by concepts such as the energy barrier (U_{eff}), blocking temperature (T_B), and quantum tunneling magnetization (QTM). Research has been conducted to improve the magnetization reversal barrier (U_{eff}) and magnetic blocking temperature (T_B), two important indicators of SMM performance. Generally, the higher U_{eff} and T_B, the better the SMM's performance. The barrier energy (U_{eff}) is formulated as $U = S^2|D|$ for integer spin and $U = (S^2 - 1/4)|D|$ for half-integer spin. Here, *S* is the ground-state spin value, and *D* is the axial ZFS parameter. Initially, the strategy was to increase *S*, but this alone had its limitations, and attention was also focused on magnetic anisotropy (*D*) [27]. Meanwhile, molecular design to improve the magnetic blocking temperature (*i.e.*, to increase the temperature), the temperature at which SMMs exhibit the aforementioned superparamagnetic hysteresis curve and behave as SMMs, has also been actively researched and reported. If uniaxiality cannot be maintained or perturbations such as transverse magnetic fields are not negligible, mixing of opposite angular momentum projections occurs, leading to degraded SMM properties due to QTM of magnetization. Therefore, precise control of both the symmetry and nature of the ligand field is essential to mitigate such perturbations and obtain better SMMs [28]. The QTM effect allows electron spins to tunnel through energy barriers via non-thermally activated pathways, thus achieving large U_{eff}. Many Ln-based SMMs were obtained since 2013 [5], and various types of the hysteresis loops were also found at zero field [29]. The most common relaxation processes in SMMs are those due to spin-phonon coupling (Auerbach, Raman, and direct processes) and quantum properties (QTM and thermally assisted-QTM). Orbach and Raman processes involve two phonons, while the direct process is assisted by a single phonon [30]. There are also promising applications, such as high-density information storage, molecular spintronics, and quantum computing. Because SMMs are also suitable for QTM between bistable states, they can be used as molecular quantum bits (qubits) with two-dimensional Hilbert spaces and can even function as quantum dots. This has the potential to advance quantum technologies, including more robust quantum information storage. Additionally, molecular spintronics, which studies spin-polarized currents for molecular information processing, could also be based on SMMs combined with supramolecular chemistry [31]. Novel molecular materials and hybrid interfaces will enable the realization of unconventional SMM-based devices. These developments are expected to add new functionality to spintronics and potentially provide novel nanomaterials for quantum computing [32].

2.2 Design Guidelines for Realizing SMM

To realize the properties of SMM, there are upper limits to the metal complexes, and it is clear that the most fundamental requirements are those related to U_{eff}, i.e., a large spin ground state (*S*) and a large uniaxial magnetic anisotropy (*D*<0). When *D* is negative, the energy difference (U_{eff}) between 0 and ±*S* represents the energy barrier to thermal reversal of the magnetic moment (Fig. 4). That is, if the thermal energy (k_BT) of the system is less than U_{eff}, the SMM cannot randomly reorient its magnetic moment and remains trapped in the potential energy minimum. Therefore, if the system is magnetized under an applied magnetic field, it will retain its magnetization even after the field is removed. The magnitude of the energy barrier to magnetization relaxation is measured by AC susceptibility measurements. In other words, it indicates that the magnetization of the SMM cannot follow a gradually increasing oscillating magnetic field [33]. This behavior is different from that observed in, for example, iron oxide particles and nanomaterials, where the standard paramagnetic characteristic curve (typically measured by DC susceptibility) shows no hysteresis after the magnetic field is removed [34]. However, in the field of lanthanide-containing SMMs, it has been suggested that a more rigorous definition of SMM would be beneficial: if there is no maximum in the imaginary part of the AC frequency-dependent magnetization, $\chi''(T)$, or if there is no clear hysteresis in the magnetic field dependence of the magnetization, then the compound should not be claimed to be an SMM [35]. Polycyanide W and Mo complexes [36,37] recording values of magnetization reversal barriers were reported (*e.g.* $\tau= \tau_0 \exp(U_{\text{eff}}/k_BT)$, with U_{eff} = 40.5 ± 0.3 cm^{-1} (58.5 ± 0.4 K) [37]).

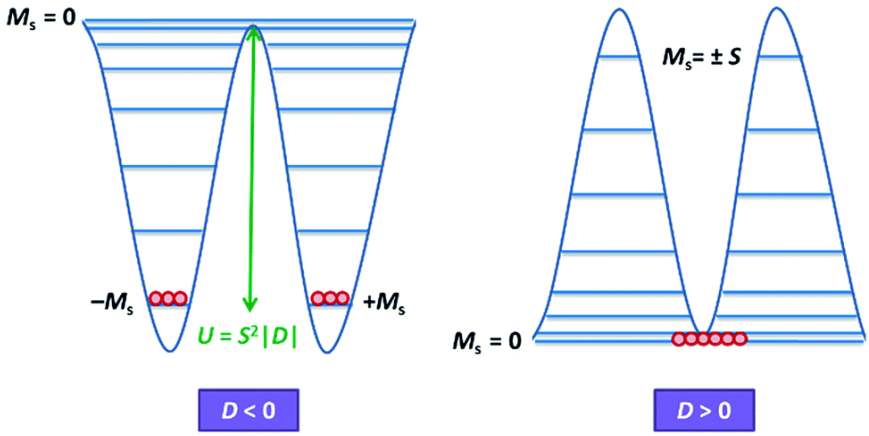

Fig. 4 *Magnetization reversal barrier, in the situation of D<0 and D>0*

2.3 Why are Cyanide-Bridged Complexes Suitable for SMM?

First, cyanide bridges promote strong magnetic interactions between metal centers. The cyanide bridge efficiently transmits magnetic interactions (ferromagnetic or antiferromagnetic) between metal ions, making it easy to form clusters with large *S*. Heterometallic cyano-bridged clusters exhibit diverse topologies, primarily dependent on (i) the coordination number and geometry of the polycyanometallate, (ii) the presence of blocking ligands that reduce the number of bridging cyanide groups, (iii) the number and spatial arrangement of labile ligands on the cationic components, and (iv) the relative charges of the components. These clusters are bonded to form closed, discrete structures in which magnetic interactions are transmitted via overlapping magnetic orbitals (super-exchanged) or directly (exchanged). Furthermore, in addition to the paramagnetic components, various additional functionalities (attachment sites) can be incorporated, such as chirality, redox activity, photochromism, or luminescence [38]. Luminescence is associated with spin states (singlet or triplet for ground or excited states) and catalysis may be controlled by valence states or spin states (odd or even numbers of electrons). The 1D or 2D bimetallic networks have been obtained, and their magnetic properties reflect the reduced dimensionality of the material. It is important to reach the '0D' or molecular level, where individual magnetic molecules can be studied in isolation. Investigating their intrinsic magnetic properties at this level is essential for designing materials in which these molecular characteristics are preserved and effectively translated into the solid state. For example, certain high-spin paramagnetic molecules could potentially become SMMs [39]. Further insights have also been gained from theoretical approaches. Studies of exchange coupling through cyanide bridges in complexes using Density Functional Theory (DFT) and empirical modeling have revealed a relationship between the exchange coupling constant and the type of spin density of the C-N bridging ligand. Using DFT values of the exchange coupling parameters, the influence of spin-orbit coupling on the isotropic and anisotropic exchange coupling in linear Cu-NC-Fe pairs has been discussed, along with their potential for ferromagnetic (or SMM) and optical magnetic materials [40]. The second advantage is structural controllability, highlighting the advantage of being able to rationally design structures with the desired dimensionality (clusters or chain-like crystal structures) through self-assembly using a building block approach. To achieve precise control over magnetic properties, topological control of the constituent metal ion building blocks is essential. Coordination chemistry offers a practical approach to finely tune the properties of SMMs, *e.g.*, as "magnets." A key consideration is to consider modules that are robust enough to maintain their structure-directing ability under assembly conditions. Another consideration is the inherent preference for specific coordination structures at the metal center and bridging ligands.

Let us illustrate the relevance of structural dimensionality with a prominent example. The magnetization dynamics of Ln containing SMMs are due to single-ion behavior. This differs from the magnetic relaxation mechanism of transition-metal SMMs, where both spin and exchange interactions simultaneously contribute to the magnetization dynamics. In contrast, in the case of metal-organic frameworks (MOFs), transition-metal-based coordination clusters act as nodes, but the high symmetry of the clusters results in weak magnetic anisotropy, and they typically do not behave as molecular nanomagnets, except for one-dimensional chain-like single-molecule magnets [41]. Third, the introduction of magnetic anisotropy has the advantage that metal ions such as Co(II), Dy(III), and Tb(III), which inherently have strong magnetic anisotropy, can be easily incorporated into the SMM structure. In order to explain magnetic properties or parameters, we also include typical examples such as 3d-4f or Ln(III) based SMMs. Among these, a Co(II) complex was reported as a new SMM characterized by metal-ligand multiple bonds. Its effective U_{eff} (*e.g.*$\tau = \tau_0 \exp(U_{eff}/k_BT)$ = 7.5 x 10^{-11} s, with U_{eff} = 297 cm^{-1} [37]) was larger than previous examples, and coercivity was also observed. The high effective relaxation barrier is attributed to the

large magnetic anisotropy due to the Kramers doublet. The introduction of strong exchange coupling provides a way to mitigate the drawbacks of the strong QTM of mononuclear SMMs [42]. Among lanthanide complexes, some with Dy(III) coordination structures close to D_{2d} symmetry exhibited SMM behavior in the absence of a static magnetic field and had large U_{eff}. Magnetic anisotropy studies using ab initio calculations revealed a clear difference between the first excited state and the experimental U_{eff} (*e.g.*τ= 3 x 10^{-13} s, with U_{eff} = 594 cm^{-1}) [43]. Furthermore, besides Dy(III), a trigonal Tb(III) complex also exhibited SMM characteristics at relatively high temperatures, with a large U_{eff} attributed to a combination of QTM, Raman, and Auerbach relaxation, and also exhibited luminescence below 100 K due to f–f electronic transitions [44].

2.4 Examples of Cyanide-Bridged SMM

First, let us introduce the early development of research into SMMs made solely of transition metals. While comprehensive reviews on the synthesis and reactivity of general 3d transition metal SMMs [45]. The synthetic schemes, routes, and preparative strategies for 3d-metal SMMs are described, along with the synthetic principles and principles behind the reactions, with particular emphasis on the choice of reactants (ligands and metal-containing starting materials).

Second, let us discuss high-performance SMMs containing Ln ions. Focusing on the 3d-4f system, which has been the subject of active research in recent years, there is a paper that explains how the huge magnetic anisotropy of lanthanides contributes to improving T_B . Approximately 387 research papers in the Cambridge Crystallographic Database report heterometallic molecular complexes containing 3d metals and lanthanide ions. Approximately 100 examples of 3d–4f SMMs were reported, with Tb(III) and Dy(III) complexes primarily exhibiting SMM properties. Less is known about magnetic coupling between 4f and 3d metals. For better SMMs, the magnetic coupling between the metal centers in the complex must be strong and ferromagnetic. This provides an isolated ground state and avoids mixing of low-lying excited states, which can lead to QTM. This is the greatest challenge for 3d–4f complexes [48]. Third, there is the development of SIMs. The concept of SMM-like behavior is not due to the magnetic interactions of the entire cluster, but rather to the (strong) magnetic anisotropy of a single metal ion, and examples of compounds have been shown later. Mononuclear SIM complexes have been reported for metal ions with large magnetic anisotropy, such as Co(II), Tb(III), and Dy(III). However, as SIM research progresses, it has been noted that there are increasing exceptions to the general rule that SMM requires negative or uniaxial magnetic anisotropy. Several complexes have been reported that exhibit slow magnetic relaxation and SIM behavior while possessing positive or easy-plane magnetic anisotropy. All of these mononuclear complexes are based on Co(II) and behave as SIM complexes only when a direct current magnetic field is applied [33]. Therefore, the situation in which magnetic anisotropy or large spin S (in bridged clusters) is considered a requirement or guideline may not continue for much longer.

3. Multi-Functions (Optical, Redox, and Magnetic) Cyanide Compounds

Cyanide-bridged coordination assemblies have recently attracted significant attention not only for their magnetic properties but also for their versatility in integrating optical switching, redox activity, and magneto-optical coupling within a single molecular architecture. Research on redox active cyanide-bridged multinuclear complexes has drawn a lot of interest in recent years [47,48]. Numerous domains, including catalysis [49], molecular devices [50], medicine [51], and energy [52,53], depend on the redox-active coordination complexes. A cyanide-bridged complex with metal centers that have redox properties is a great platform for studying intramolecular electron transfer and the related physical features because of potent electron-delivering capabilities of cyanides. Numerous cyanide-bridged complexes having redox properties have been created, described, and their characteristics, including electrical conduction, magnetism, and metal-metal charge transfer (MMCT), have been examined since the discovery of the first cyanide-bridged complex, Prussian Blue, in the 18th century [54,55]. There is increased interest in designing novel heterometallic complexes for operations involving photoinduced atom transfer. As a light absorber and oxygen atom transfer agent, one method is to use self-assembly processes to connect a polypyridine to a metal oxo fragment. Three metal centers forming a V-shaped complex, $[CN–Pt(II)\text{-}cis\text{-}Ru(II)(phen)_2Cl_2(DMSO)]_2$, were synthesized using cyanide bridges to connect two $PtCl_2(DMSO)$ units to a central Ru(II) ion [56] (Figure 5). The two Pt(II) are given a square planar coordination geometry by a coordinated DMSO which is *trans*-position with cyanide bridge and two Cl ligands that are trans to one another. With a sharp decrease in luminous intensity, the Ru^{II} -diimine chromophore's MLCT (metal-to-ligand charge transfer) transition moves from 452 to 384 nm, and the emission in the MLCT region moves from 621 to 595 nm. This blue-shift is accompanied by a significant variation in emission intensity, particularly upon interaction with specific substrates as observed in spectrofluorimetric titrations. For peptides and amino acids that include sulfhydryl, the complex is the first luminous chemo dosimeter that is selective. On the donor using different polypyridyl ligands that is chromotropic, the fluorimetric responses of the ensembles may be adjusted. Carbonyl chromophore of Ru diimine and connecting cyanide and anions of cyanide-metalate are used in the study to show how to create homo- and heterometallic complexes.

J. of Sustainable Materials Processing and Management Vol. 6 No. 1 (2026) p. 1-19

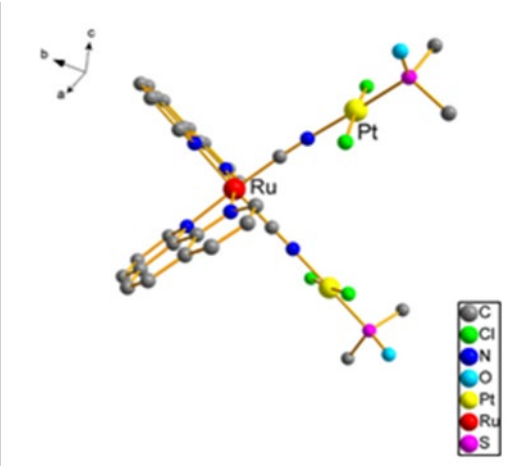

Fig. 5 *Trinuclear complex cis(phen)2Ru(II) [CN–Pt(II)Cl2(DMSO)]2*

The use of Re(I) diimine tricarbonyl chromophores to generate homo and heterometallic complexes and cyanide and anions of cyanometallate has been investigated [57]. Cyanide-bridged dirhenium compounds formulated as $[\{Re(CO)_3(diimine)\}_2CN]^+$ are produced by reacting $[Re(CO)_3(diimine)(H_2O)]^+$ (where diimine represents 2,2′-bipyridine or phenanthroline) with dicyanoargentate anions. Furthermore, a heterobimetallic Re(I)–Au(I) complex, $[\{Re(CO)_3(phen)\}AuNC(PPh_3)]^+$, is synthesized by employing the neutral metallo-ligand $[Au(PPh_3)(CN)]$. Additionally, a phosphine-substituted derivative, $[\{Re(CO)_2(phen)(PPh_3)\}_2CN]^+$, can be obtained by substituting the axial carbonyl ligands of the parent dirhenium complex with triphenylphosphine. Furthermore, cyanide complexes of Au, Pt and Fe are used to create the higher nuclearity aggregates $[\{Re(diimine)\text{-}(CO)_3NC\}xM]^{m+}$,where M = Au, x = 2, 5 and 6; Pt, x = 4, 7 and 8; Fe, x = 6, 9 and 10). The study showed that the center pieces are polydentate, which permits target assemblies to have different unclarities. With a negligible heterometal contribution, the Re(I) elements of these complexes control their optical characteristics. These compounds' luminescence is linked to electronic transitions that are primarily of the triplet-MLCT nature. These compounds' electrochemical activity demonstrates irreversible Re(I) ion oxidation and a nearly reversible redox reaction of the $[Fe(II/III)\ (CN)_6]^{4-/3-}$ groups. Optically, the complexes display characteristic Re(I)-based MLCT absorption bands and corresponding emission profiles that mirror the excitation spectra [57].

A two-dimensional coordination polymer based on Cu/Ni, $[\{Cu(II)(4,4'\text{-dipy})_2\}\{Ni(CN)_4\}]$ (hereafter referred to as CP-1), has been reported as a potential co-catalyst supported on TiO_2 for hydrogen evolution under UV irradiation [58]. In this compound, dipy represents dipyridyl. Compared with pure CP-1 and TiO_2, the CP-1/TiO_2 composite exhibits significantly enhanced hydrogen production, indicating that the improved photocatalytic activity is associated with efficient separation of photogenerated electron–hole (e^-/h^+) pairs. Different CP-1 loadings (2.5, 5, and 7.5 wt%) in CP-1/TiO_2 composites were evaluated for photocatalytic hydrogen generation in a 5 vol% glycerol/water mixture. The composite containing 5 wt% CP-1/TiO_2 showed the highest hydrogen evolution rate of 9.2 mmol h^{-1} g^{-1}, outperforming the other compositions in catalytic efficiency [58]. Three cyanide-bridged trinuclear complexes that are redox active are *trans*-$Ru(DMAP)_4$ $(\mu\text{-}CN)^{2-}[MPF_6(PY_5Me_2)]_2]_4$ (M = Co, Ni, Cu) {DMAP = pyridine-4-dimethylamino, PY_5Me_2 represents 2,6-bis(1,1-bis(2- ethyl- pyridyl-pyridine}, were created by Zhu *et al* [59]. The compounds DMAP = pyridine-4-dimethylamino, PY_5Me_2 = 2,6-bis(1,1-bis(2-thyl- pyridyl-pyridine were prepared and characterized using cyclic voltammetry, magnetic measurement, elemental analysis, XRD, and infrared spectrophotometer. The compound trans-$Ru(DMAP)_4(\mu\text{-}CN)^{2-}[CuPF_6(PY_5Me_2)]_2]_4$ exhibits an unusual disordered conformation as a result of the Cu(II) ion's Jahn-Teller distortion. The Co and Ni centers in *trans*-$Ru(DMAP)_4$ $(\mu\text{-}CN)^{2-}[CoPF_6(PY_5Me_2)]_2]_4$ and *trans*-$Ru(DMAP)_4(\mu\text{-}CN)^{2-}[NiPF_6\ (PY_5Me_2)]_2]_4$ are redox-active, with the exception of the Ru center, according to cyclic voltammetry. According to magnetic studies, *trans*-$Ru(DMAP)_4(\mu\text{-}CN)^{2-}[NiPF_6\ (PY_5Me_2)]_2]_4$ has a very weak anti-ferromagnetic coupling constant. *Trans*-$Ru(DMAP)_4$ $(\mu\text{-}CN)^{2-}$ $[Cu\ PF_6\ (PY_5Me_2)]_2]_4$ is simply paramagnetism, and *trans*-$Ru(DMAP)_4$ $(\mu\text{-}CN)^{2-}[Co\ PF_6\ (PY_5Me_2)]_2]_4$ has paramagnetism with a substantial magnetic anisotropy of Co(II) ions, as evidenced by the deviation of the $\chi_M T$ product at low temperatures [59].

The DC magnetic study of *trans*-$Ru(DMAP)_4(\mu\text{-}CN)^{2-}[NiPF_6(PY_5Me_2)]_2]_4$ and *trans*-$Ru(DMAP)_4(\mu\text{-}CN)^{2-}[CuPF_6(PY_5Me_2)]_2]_4$. Three-dimensional porous coordination polymers, $1{\cdot}3CHCl_3$ and $1{\cdot}2.5CH_2Cl_2$, were synthesized and characterized using thermogravimetric, magnetic, optical, calorimetric, and X-ray diffraction analyses [60]. The 3D polymer $1{\cdot}2.5CH_2Cl_2$ exhibits a two-step incomplete spin crossover behavior, whereas $1{\cdot}3CHCl_3$ shows a one-step incomplete transition centered at $T_1/_2 \approx 85$ K. Owing to the presence of cavities capable of accommodating dichloromethane or chloroform molecules, these materials display different color variations. Cryogenic optical microscopy was used to investigate the spatiotemporal features of the thermal transitions at the

single-crystal level for both compounds. The results indicate that these polymers may serve as recyclable materials for gas sensing and chemical storage through modulation of their magnetic and optical properties via host–guest interactions within the crystal cavities. The thermal hysteresis loops observed in magnetic susceptibility measurements are consistent with the heat capacity anomalies detected in calorimetric studies [60].

4. Ligand Field Theory Vs DFT for Multi-Functional Cyanide Complexes

4.1 Why are Theoretical Calculations Important?

As for "multi-physical properties", beside direct SMM functions, we want to include them from the viewpoint of designing structures and electronic states. In experiments, properties such as magnetic susceptibility, magnetic anisotropy (*e.g.* ZFS), optical absorption spectra, and redox potentials of transition metal complexes are observed. Theoretical calculations are extremely useful for elucidating the electronic states (such as d-orbital configuration, inter-orbital transitions, spin-orbit coupling, and metal–ligand bond covalency/hybridization) from which these properties arise. For experimental results that reflect complex effects like multiple structures, spin-orbit coupling, and charge transfer—such as metal L-edge X-ray absorption spectroscopy and resonant inelastic X-ray scattering spectra—simulation *via* high-level theoretical calculations is indispensable for detailed interpretation and assignment [61]. Furthermore, quantitative calculations such as DFT and Time-Dependent DFT (TD-DFT) serve as powerful tools to systematically understand how slight chemical modifications of ligands (*e.g.*, the binding mode of CNS^- ligands) affect the geometric structure, spin state, and absorption spectrum of the complex [62], or to disentangle complex phenomena where spin crossover (SCO) and electron transfer occur simultaneously [62, 63]. Additionally, since the chemical space of transition metal complexes is vast—often termed a "combinatorial explosion"—due to the combinations of metals, ligands, spin states, and oxidation states [64, 65], searching for physical properties experimentally by trial and error is inefficient. By using theoretical calculations (especially high-throughput virtual screening and machine learning), it is possible to establish design guidelines (e.g., predicting that a specific ligand/structure will yield desired magnetic or optical properties), thereby dramatically accelerating the process of rationally synthesizing and exploring complexes with targeted functions [66]. In other words, in coordination chemistry, the concerted "experiment–theory" approach—such as utilizing huge experimental crystal structure databases (like the Cambridge Structural Database) as training data for machine learning models (e.g., Graph Neural Networks) to predict the coordination structure and properties of novel complexes with high speed and accuracy [64]—dramatically improves the efficiency of material design. However, only a limited number of experimental–computational studies have been reported so far. In fact, cyanide-based materials, due to their robust bonding and unique electronic properties like strong ligand field characteristics and σ-donor/π-acceptor nature [65, 66], serve as platforms for extremely diverse functional materials, including molecular adsorption/separation and energy storage, in addition to the SCO, molecular magnetism, and photophysical properties discussed in this review [66]. Theoretical calculations play an increasingly significant role in understanding and designing these complex functions (*e.g.* the coexistence of SCO and electron transfer) [63, 66].

4.2 Qualitative Understanding Via Ligand Field Theory (LFT)

LFT begins with the framework that the d-orbitals of a metal ion undergo energy splitting due to the ligand field (the electric field/bonding exerted by ligands on the metal). For example, in an octahedral field, this is treated as the splitting of $d(t_{2g})/d(e_g)$ orbitals ($10Dq$). The cyanide (CN^-) is generally known as a ligand that provides a "strong ligand field," and a typical example is that it often induces a low-spin state (ligand field splitting > pairing energy) in systems like $[Fe(CN)_6]^{4-}$. However, this intuitive picture of LFT is not always correct; for instance, it is known that in the $[Cr(CN)_5]^{3-}$ complex, the high-spin state (S=2) becomes the ground state [67]. Furthermore, even in systems where π-back-donation is expected in a d^6 system, such as the Fe(II) porphyrinate complex $[Fe(TPP)(CN)]^-$, there are reports of cyanide ligands inducing SCO behavior (meaning the low-spin state is not stable) [68], demonstrating the diversity of cyanide ligand behavior. When magnetic anisotropy constants D and E are observed, intuitive understanding is possible within LFT. For example, if the orbital angular momentum remaining on the metal ion is large (orbital degeneracy is not fully lifted, or orbital mixing is small), SOC acts relatively strongly, which is explained as resulting in large magnetic anisotropy. The symmetry of the coordination structure (e.g., trigonal, square planar, pentacoordinate) affects orbital degeneracy/mixing, allowing qualitative prediction of the sign (easy-axis vs. easy-plane) and magnitude trends of D. For example, in $5d^3$ Re(IV) complexes, the classical LFT prediction (based on the perturbation expression derived by Abragam and Bleaney) that axial compression leads to $D < 0$ and elongation to $D > 0$ has been supported by ab initio calculations [69].

Furthermore, LFT-based interpretations—such as the ligand position (axial vs. equatorial) systematically changing the d-orbital splitting pattern and determining the sign of D (e.g., in Re(IV) complexes, ligand substitution in the equatorial plane systematically yields a negative D value, whereas substitution at the axial positions leads

to a positive D value)—can serve as powerful design guidelines [64]. Similarly, in lanthanide (4f) SMMs, the magneto-structural correlation between coordination structure and magnetic anisotropy is extremely important. Theoretical studies on Dy(III)N_8 complexes -like porphyrin ligand complexes- have shown that slight distortions in coordination geometry (D_{2d} vs. C_{2v} symmetry) due to K^+ ion intrusion, or changes in the ligand torsion angles, have a decisive effect on the magnetic anisotropy barrier (U_{cal}). In particular, the LFT design guideline that ideal square-antiprismatic (D_{4d}) symmetry stabilizes the pure $|m_j| \geq \pm 15/2 >$ ground state and maximizes anisotropy is supported by computational chemistry [70].

Summarizing the pros and cons of LFT: its advantage is that it provides a very intuitive and clear physical picture (d-orbitals, splitting, pairing, orbital degeneracy, spin states, etc.) for coordination chemists, serving as a clue to discuss experimental data (d-d absorption, magnetic measurements, *etc.*) from the perspective of "orbital configuration" or "coordination structure." For example, LFT methods like the Angular Overlap Model serve as effective "interpretive tools" that quantitatively reproduce the effect of ligand differences (Cl^- vs. SCN^-) on D values (SCN^- yielding more negative D) in Cr(II) chain complexes [71]. Additionally, the LFT framework is applicable not only to traditional coordination complexes like $[Cu(CN)_4]^-$ but also to highly covalent organometallic complexes like ferrocene $[Fe(Cp)_2]$, where Cp represents cyclopentadienyl, providing a unified conceptual basis for interpreting ligand bonding (e.g., π-donating or δ-accepting nature of Cp^-) [69]. However, while the intuitive picture of LFT is powerful, it is not omnipotent. For instance, despite cyanide being a typical strong-field ligand, it has been reported that the $[Cr(CN)_5]^{3-}$ complex experimentally has a high-spin (S=2) ground state. This phenomenon is difficult to explain solely with the LFT picture (orbital interaction), and DFT calculations were the first to show that it is due to Coulomb repulsion between ligands—an element not considered in LFT—exceeding the orbital interaction energy [64]. Similarly, the fact that $[Fe(TPP)(CN)]^-$ exhibits SCO is difficult to predict with simple LFT pictures [69]. Thus, it is difficult to quantitatively treat splitting energies ($10Dq$ or B, C parameters), SOC, orbital mixing, electron correlation, metal-ligand covalency, and multiple structures accurately.

Fundamentally, LFT is an empirical approach where parameters are obtained by comparison with experimental data, and it has a strong aspect of being an "interpretive tool" rather than a "predictive tool" [61]. Especially in systems where spin-orbit coupling is extremely strong, such as 5d transition metals (e.g., Re(IV)), the static picture of LFT (transitions within the same spin state) is insufficient for accurate evaluation of D values; more advanced ab initio calculations (like CASPT2) that consider spin-flip excitations (transitions between different spin states) and dynamic correlation become indispensable [63]. Also, in "ultra-covalent" regions like $[Ni(Cp)_2]^{2+}$, metal d-orbital and ligand orbital mixing becomes too strong, breaking the premise of LFT that the "d^n configuration is maintained" (protection by the Pauli shield), thus reaching the limit of LFT applicability [72]. Therefore, in systems with strong electron correlation, polynuclear systems, or systems with metal-metal bridging/conductivity, LFT alone becomes insufficient.

4.3 Quantitative Evaluation Via DFT

Next, as a quantitative approach, we explain calculations using DFT [73]. DFT is a first-principles calculation method that determines the total energy of a system using electron density as the main variable, and is practically applied to various metal complexes and material systems. It is expected to be a model compatible with traditional LFT formalism while being a "predictive theory" that does not require empirical parameters like LFT [74,75].

4.3.1 Calculation of Magnetic Parameters

Specific approaches are used when calculating magnetic parameters. For example, for the exchange interaction constant J, the "Broken-Symmetry (BS) approach" is used to calculate the magnetic coupling strength between different metal spins, which is one of the most practical methods for multicenter transition metal complexes. In this method, the energy difference between different spin configurations (such as the ferromagnetic state and the lowest spin state) is determined, and the J value is calculated from this energy difference and the expectation value of the spin operator using the Yamaguchi formalism [76,77].

$$J = \frac{2(E_{LS} - E_{HS})}{S^2{}_{HS} - S^2{}_{LS}} \quad (1)$$

Regarding the magnetic anisotropy constant D, the ZFS tensor can be quantitatively evaluated using DFT-based approaches (such as the Pederson-Khanna method) that introduce SOC as a second-order perturbation [78]. Especially in polynuclear systems like Fe(III)-CN-Ni(II), it has been pointed out that not only the anisotropy derived from the orbital angular momentum of Fe(III), but also the combination with the ZFS (D value) of the Ni(II) site itself can significantly enhance or cancel the overall magnetic anisotropy [78, 79]. Although ZFS mainly originates from the spin-orbit term, the spin-spin interaction term can reach 20-30% of the total D value depending on the system, sometimes making a non-negligible contribution [78]. Calculation of optical and

electrochemical properties is similarly possible. As an example, electronic absorption spectra are predicted using TD-DFT for d-d transitions and LMCT/MLCT transitions of metal complexes [80]. However, TD-DFT calculations are highly dependent on the functional, especially in describing CT excitations, and caution is required as GGA (Generalized Gradient Approximation) and some hybrid functionals may predict non-physical low-energy "ghost states" [81]. For redox potentials, the redox behavior after coordination environment changes is calculated using Gibbs free energy differences by DFT and solution phase models [81]. In this context, it has been reported that the "choice of solvation model" has a decisive impact on prediction accuracy, more so than the choice of functional or basis set. Especially for complexes with high charges, errors in implicit solvation models tend to be large [81].

4.3.2 Pros and Cons of DFT

Thus, DFT is extremely powerful for theoretically elucidating and predicting "magnetic and optical/electrochemical multifunctionality." For example, in research on Ru(II) pyridyl imidazole complexes, DFT and TD-DFT calculations have been used to rationally explain experimentally observed changes in redox potentials, absorption spectra, and photophysical properties (excited states) associated with changes in protonation state (acid dissociation constant, p*K*a) [82].

Summarizing the pros and cons of DFT: its advantages are relatively high quantitative accuracy, versatility, and the ability to handle coordination structure, electronic state, magnetism, absorption spectra, reduction potentials, etc., within the "same computational system" [83]. Limitations include that the choice of functional greatly affects the results. For example, in J value calculations, GGA functionals (such as the Predew-Burke-Ernzerhof functional) tend to overestimate antiferromagnetic coupling due to delocalization of electrons caused by self-interaction error [84]. On the other hand, hybrid functionals (B3LYP, PBE0, *etc.*) tend to overcorrect this error by introducing exact exchange, biasing results towards ferromagnetism [85]. As a challenge for TD-DFT, range-separated hybrid functionals may be required for describing CT excitations [86]. Also, while ligand field splitting ($10Dq$) can be calculated relatively accurately, there is a tendency to systematically underestimate Racah parameters (B, C) representing inter-electron repulsion, which affects energy predictions of spin-forbidden transitions [74]. As a more fundamental issue, accuracy decreases in systems where the effects of "delocalization error" and "static correlation error" inherent in DFT become pronounced [73].

Furthermore, there are limits to accuracy and reliability in strongly correlated electron systems (*e.g.*, systems involving multiple/static correlation of 3d transition metals), systems with large SOC effects of heavy elements, and polynuclear/conductive/metal-metal bonded systems. Particularly in systems with large magnetic anisotropy (D) (*e.g.*, d^2, d^4 complexes or mononuclear SMMs), DFT tends to significantly underestimate D values because the multireference character of the ground state becomes strong [78]. Also, current approximate functionals may give apparently correct values for "wrong physical reasons" due to accidental cancellation of errors, so careful interpretation of results is necessary [75]. Finally, there is the reality that computational cost and pre-processing (structure optimization, examination of ligand-to-metal arrangement, etc.) are "heavy" for exploring large structural spaces in the complex design stage.

4.4 Complementary Use of LFT and DFT

As mentioned above, LFT and DFT each have their pros and cons, but practically, the flow of "first obtaining intuition with LFT, then quantitatively verifying/predicting that hypothesis with DFT" is very effective. As a further advanced complementary approach, "DFT-based Ligand Field Theory (LFDFT)," which derives LFT parameters themselves *ab initio* based on DFT calculations, has also been developed. In this method, the energies of Slater determinants of the system are calculated by DFT, and the parameters of the ligand field Hamiltonian ($10Dq$, B, C, *etc.*) are determined to reproduce these energies. The advantage of this approach is that "dynamic correlation" of electrons can be effectively incorporated via DFT calculation, and "non-dynamic correlation" via the LFT framework (and multiplet configuration interaction calculation). Thus, DFT calculation serves as a powerful bridge connecting the intuitive picture of LFT with quantitative accuracy [74].

For example, in research targeting the magnetic anisotropy of Fe(III)-CN-M(II) (M=Cu, Ni) type cyanide-bridged SMMs, this very LFDFT model is used. In this approach, the effects of Jahn-Teller distortion and symmetry distortion on spin-orbit coupling are quantitatively evaluated by DFT calculations, quantitatively supporting hypotheses that were intuitive pictures of LFT, such as "enhancement of anisotropy by tetragonal field (^2E_g ground state)" and "reduction of anisotropy by trigonal distortion" [72, 76, 79]. On the other hand, approaches using DFT alone may have issues in quantitative evaluation of magnetic anisotropy such as the ZFS tensor (D^{SO}). For instance, systematic studies using $M(acac)_3$ (M = V, Cr, Mn, Fe, Mo) complexes show that while DFT-based perturbative approaches (such as the standard Pederson-Khanna method and its natural orbital-based refinement) reproduce the overall trend of the D tensor, they systematically underestimate the contribution of specific electronic excitations, particularly those from singly occupied to unoccupied orbitals, compared to ab initio calculations (CASSCF/MRMP2) [78]. This error is accidentally cancelled in d^3 and d^5 configurations but becomes pronounced in d^2 and d^4 configurations, suggesting that DFT is not omnipotent and that verification with LFDFT or ab initio

calculations is important [78]. Similar complementary approaches of theory and experiment are essential for understanding cyanide-bridged multifunctional materials containing lanthanides (4f metals). In the case of lanthanide SMMs, unlike 3d metals, SOC is dominant over ligand field effects, and magnetic anisotropy design requires these theoretical guidelines (*e.g.*, oblate/prolate rules) [83]. A review by Chorazy *et al.* on luminescent Ln-SMMs shows examples in d-f cyanide heterometallic systems where *ab initio* calculations are used complementarily with high-resolution emission spectra to determine ground multiplet splitting by ligand field and contribute to elucidating magnetic relaxation mechanisms [83]. In practice, LFT is extremely effective for "relatively simple systems with mononuclear/uniform coordination," but quantitative calculations using DFT (or LFDFT and higher-level multiplet wave function methods) are almost essential for "designed systems with complex multifunctionality such as polynuclear, bridged ligands, magnetic coupling, conductivity, photocatalytic properties." Especially in the design of spin-crossover materials, the combination of the basic LFT concept of d^6 low-spin states due to strong ligand fields like cyanide and DFT calculations to evaluate the effect of slight differences in ligands and structure on transition behavior has become a standard approach [66].

5. DFT for Parameters of SMMs

5.1 Rational Design of SMMs and DFT Calculations

SMMs have attracted significant attention since the first report of magnetic hysteresis at the single-molecule level in $[Mn_{12}O_{12}(OAc)_{16}(H_2O)_4]$ (commonly known as Mn_{12}) in 1993 [84]. This interest stems from their fundamental magnetic properties, particularly phenomena such as the QTM and quantum phase interference [85,86]. Furthermore, vigorous research continues due to their potential applications, including the demonstration of magnetic memory using SMMs anchored on surfaces [87,88], theoretical proposals for their use as qubits [89] with experimental verification [90], and the development of molecular spintronics. Improving the effective energy barrier for magnetization reversal (U_{eff}) and the blocking temperature (T_B), which are performance metrics for SMMs, remains a critical challenge in this field. Early research focused on transition metal clusters represented by Mn_{12} [84], where the prevailing synthetic strategy was to maximize the ground spin state S based on the relationship $U_{eff} = |D|S^2$. However, it became recognized that achieving both a large S and a large axial magnetic anisotropy constant D simultaneously is difficult [85]. The discovery of Ln-based SMMs (SIMs) in 2003 marked a turning point. The mainstream approach for designing high-performance SMMs shifted toward utilizing the intrinsic large magnetic anisotropy of f-electrons, specifically through the precise control of D. In this rational design process, theoretical calculations, represented by DFT, have become indispensable tools for synthetic chemists to elucidate the correlation between molecular structure and magnetic parameters (J and D) and to provide powerful design guidelines [85-90].

5.2 Calculation of Exchange Interaction Constants (J)

In polynuclear SMMs, the ground spin state S is determined by the exchange interaction constant J between spin centers. Predicting the sign (ferromagnetic $J > 0$ / antiferromagnetic $J < 0$) and magnitude of J is essential for designing clusters with the intended S. The BS method based on DFT (DFT-BS) has been established as a standard and powerful technique for estimating J. This method calculates J from the energy difference (E_{HS}-E_{BS}) between the high-spin (HS) state and the BS state, in which the spin projection is artificially flipped. The DFT-BS method has been widely used to predict the sign and magnitude of magnetic interactions mediated by diverse bridging pathways, such as oxo, hydroxo, cyanide, or various organic ligands [91–93]. Through these computational chemical methods, the influence of structural factors—such as metal-metal distances and angles, the protonation state of bridging ligands, and ligand substituent effects—on the J value has been analyzed in detail [94-96]. Furthermore, in recent years, the scope of its application has expanded significantly. For instance, the DFT-BS method was applied to analyze extremely weak super exchange interactions mediated by hydrogen bonding networks in crystals of mononuclear Cu(II) complexes [94]. Their study demonstrated that small J values, such as +5.53 cm^{-1} (ferromagnetic) and -2.21 cm^{-1} (antiferromagnetic), arise through water-mediated O–H···Br or N–H···O hydrogen bonding pathways. Thus, the DFT-BS method serves as a powerful computational tool for modeling diverse intramolecular and intermolecular interaction pathways and elucidating their magnetic contributions.

5.3 Calculation of Magnetic Anisotropy Constants (D)

The most critical factor directly determining the energy barrier U_eff of an SMM is the magnetic anisotropy constant D (or ZFS). Since D originates primarily from SOC, its calculation is more complex than that of J. In particular, the origin of D in d-electron system (transition metal) SMMs is a difficult problem involving competing factors, and its theoretical framework has been built alongside the development of electronic state theory for transition metal ions [96,97]. A detailed theory for calculating ZFS tensors using high-spin Fe(III) complexes (S =

5/2) as model systems has been developed based on long-standing insights into EPR spectroscopy and electronic state theory [98,99]. These theories [100], based on the effective Hamiltonian method [101,102], showed that the value of D is governed not only by contributions from excited states with the same spin multiplicity (S = 5/2) mixing with the $^6A_1$ ground state via SOC, but also significantly by second-order contributions from excited states with different spin multiplicities (S = 3/2, i.e., S − 1 states).

Furthermore, they demonstrated that the sign and magnitude of D are strongly influenced by ligand field symmetry (structural distortion), "anisotropic covalency" (*e.g.*, differences in the degree of metal-ligand hybridization between t_2 and e orbitals), contributions from charge transfer (CT) excited states, and the SOC of the ligand atoms themselves [96]. Thus, precise prediction of D in d-electron systems requires the accurate evaluation of all these contributions.

On the other hand, the situation differs for Ln SMMs possessing f-electrons. Due to the localization and strong electron correlation of f-electrons, as well as SOC that is far larger than in d-electron systems, standard DFT cannot accurately describe their magnetic anisotropy. Therefore, in lanthanide systems, multi-reference computational methods such as Complete Active Space Self-Consistent Field (CASSCF) calculations, followed by Restricted Active Space State Interaction methods, have become the standard approach for estimating crystal field parameters corresponding to D.

6. Computational Challenges and Future Perspectives

As reviewed in this article, cyanide-bridged coordination polymers and polynuclear complexes have established a unique position as platforms for multifunctional materials. They possess not only magnetic properties but also optical and electrochemical functionalities, owing to their structural design flexibility and robust bonding characteristics [1,48]. Research on SMMs has undergone a paradigm shift from the pursuit of high spin states using polynuclear clusters, such as Mn12, to SIMs that utilize the strong magnetic anisotropy D of lanthanides or low-coordinate transition metals. This shift has led to remarkable progress in improving the blocking temperature T_B [27, 33]. In the design of these materials, theoretical computational chemistry is no longer merely a tool for the *post-facto* interpretation of experimental results; it has become an indispensable partner for property prediction and rational design. As discussed in previous Sections 4 and 5, DFT methods demonstrate great power in the quantitative evaluation of exchange interactions J and the prediction of multifunctionality (such as redox potential and optical absorption). However, challenges remain in the accurate evaluation of magnetic anisotropy D, which is central to SMM performance, particularly in systems containing heavy elements [73,77].

The major challenges and future perspectives in SMM research and computational chemistry can be summarized in the following three points. The first challenge is the accurate and efficient description of 4f electron systems containing lanthanides. While lanthanide-based SMMs currently represent the mainstream of high-performance SMMs, standard DFT is insufficient to describe their strong spin-orbit coupling and electron correlation. Consequently, multi-reference computational methods, such as CASSCF, are required [87]. However, high-precision calculations that include dynamic correlation and contributions from 5d orbitals are extremely computationally expensive, hindering their application to larger integrated systems or complex coordination environments [87]. The establishment of new theoretical methods or approximation techniques that resolve this trade-off between "computational accuracy" and "computational cost" is eagerly awaited.

The second challenge is the dynamic simulation of magnetic relaxation. The T_B, which determines the practical performance of an SMM, depends strongly not only on the height of the energy barrier (U_{eff}) but also on relaxation processes (such as Raman processes) driven by coupling with the QTM and phonons (lattice vibrations) [27]. As demonstrated with Dy-based SIMs [103], the theoretical treatment of spin–phonon coupling is indispensable for designing truly high-performance SMMs capable of retaining magnetization at high temperatures. Future efforts will require the development of computational methods that dynamically model the influence of molecular and lattice vibrations on spin states, going beyond static electronic state calculations. The third perspective is the acceleration of material exploration through integration with Materials Informatics. The "combinatorial explosion" resulting from the vast combinations of transition metals and ligands makes exhaustive experimental exploration difficult, but it presents a significant opportunity for data-driven science [64]. As mentioned in Section 4, applying machine (deep) learning (*e.g.*, Graph Neural Networks) using accumulated crystal structure databases and DFT calculation results as training data makes it possible to rapidly screen candidate molecules with desired magnetic and optical properties from a vast chemical space [64,65].

In conclusion, the field of cyanide-bridged compounds is transitioning to a new phase toward next-generation device applications, such as qubits for quantum computing [32] and molecular spintronics [33], driven by the fusion of precise synthetic chemistry, advanced theoretical calculations, and data science. Complementary collaboration between experimentalists and theorists, approaching the subject from the perspectives of both static structure and dynamic relaxation, will be the key to further breakthroughs in this field.

Acknowledgement

During the preparation of this manuscript, the authors used Gemini 3 (Google) to improve the language and readability. The authors have reviewed and edited the output and take full responsibility for the content of this publication.

Conflict of Interest

The authors declare no conflicts of interest.

Author Contribution

***Conceptualization**, T.A.; **data curation**, A.U., T.A; **writing—original draft preparation**, A.U, A.K., H.S.; **writing—review and editing**, D.N., T.A.*

Abbreviations

The following abbreviations are used in this manuscript:

Abbreviation	Full name
D	dimension, dimensional
SMM	Single-Molecule Magnet
SCM	Single-Chain Magnet
SIM	Single-Ion Magnet
Ln	Lanthanide
XRD	X-ray Diffraction
SIM	Single-Ion Magnet
ZFS	Zero-Field Splitting
QTM	Quantum Tunneling of Magnetization
TA-QTM	Thermally Assisted Quantum Tunneling of Magnetization
DFT	Density Functional Theory
TD-DFT	Time-Dependent Density Functional Theory
LFT	Ligand Field Theory
LFDFT	DFT-based Ligand Field Theory
SOC	Spin-Orbit Coupling
SCO	Spincross over
BS	Broken-Symmetry
MOF	Metal-Organic Framework
MMCT	Metal-Metal Charge Transfer
MLCT	Metal-to-Ligand Charge Transfer
DMSO	Dimethyl sulfoxide
Cp	Cyclopentadienyl
TPP	Tetraphenylporphyrin
GGA	Generalized Gradient Approximation
CASSCF	Complete Active Space Self-Consistent Field
RASSI	Restricted Active Space State Interaction

References

[1] Aguilà, D., Prado, Y., Koumousi, E. S., Mathonière, C., & Clérac, R. (2016). Switchable Fe/Co Prussian blue networks and molecular analogues. *Chemical Society Reviews*, *45*(1), 203-224. https://doi.org/10.1039/C5CS00321K

[2] Wang, S., Ding, X. H., Zuo, J. L., You, X. Z., & Huang, W. (2011). Tricyanometalate molecular chemistry: A type of versatile building blocks for the construction of cyano-bridged molecular architectures. *Coordination chemistry reviews*, *255*(15-16), 1713-1732. https://doi.org/10.1016/j.ccr.2011.01.057

[3] Rebilly, J.-N., & Mallah, T. (2006). Synthesis of single-molecule magnets using metallocyanates. *Struct. Bond.*, 122, 103–131. https://doi.org/10.1007/430_032

[4] Wang, S., Ding, X.-H., Li, Y. H., & Wuang, W. (2012). Dicyanometalate chemistry: A type of versatile building block for the construction of cyanide-bridged molecular architectures. *Coord. Chem. Rev*., 256, 439–464. https://doi.org/10.1016/j.ccr.2011.10.029

[5] Korzeniak, T., Nowicka, B., & Sieklucka, B. (2018). Hybrid organic–inorganic cyanide-bridged networks. In V. Chandrasekhar & F. Pointillart (Eds.), Organometallic magnets. *Topics in Organometallic Chemistry*, 64, 1–34. https://doi.org/10.1007/3418_2018_2

[6] Ohba, M., & Ōkawa, H. (2000). Synthesis and magnetism of multi-dimensional cyanide-bridged bimetallic assemblies. *Coord. Chem. Rev.*, 198, 313–328. https://doi.org/10.1016/S0010-8545(00)00233-2

[7] Atanasov, M., Comba, P., Hausberg, S., & Martin, B. (2009). Cyanometalate-bridged oligonuclear transition metal complexes—Possibilities for a rational design of SMMs. *Coord. Chem. Rev*., 253, 2306–2314. https://doi.org/10.1016/j.ccr.2009.01.033

[8] Ni, Z.-H., Xu, L., Li, N., & Zhang, L.-F. (2017). A cyanide-bridged one-dimensional CrIIICoII metamagnet based on the trans-dicyanidechromate (III) building block. *Inorg. Chim. Acta*, 462, 204–208. https://doi.org/10.1016/j.ica.2017.03.034

[9] Zhao, J.-P., Yang, Q., Liu, Z.-Y., Zhao, R., Hu, B.-W., Du, M., & Bu, X.-H. (2012). A unique substituted Co(II)-formate coordination framework exhibits weak ferromagnetic single-chain-magnet like be-havior. *Chem. Commun*., 48, 6568–6570. https://doi.org/10.1039/C2CC31204B

[10] Liu, S.-J., Han, S.-D., Zhao, J.-P., Xu, J., & Bu, X.-H. (2019). In-situ synthesis of molecular magnetorefrigerant materials. *Coord. Chem. Rev.*, 394, 39–52. https://doi.org/10.1016/j.ccr.2019.05.009

[11] Nihei, M., Okamoto, Y., Sekine, Y., Hoshino, N., Shiga, T., Liu, I.-C., & Oshio, H. (2012). A light-induced phase exhibiting slow magnetic relaxation in a cyanide-bridged [Fe4Co2] complex. *Angew. Chem. Int. Ed*., 51, 6361–6364. https://doi.org/10.1002/anie.201202225

[12] Pichon, C., Suaud, N., Duhayon, C., Guihéry, N., & Sutter, J.-P. (2018). Cyano-bridged Fe(II)–Cr(III) single-chain magnet based on pentagonal bipyramid units: On the added value of aligned axial anisot-ropy. *J. Am. Chem. Soc.*, 140, 7698–7704. https://doi.org/10.1021/jacs.8b03891

[13] Bousseksou, A., Molnár, G., Salmon, L., & Nicolazzi, W. (2011). Molecular spin crossover phenomenon: recent achievements and prospects. *Chem. Soc. Rev.*, 40, 3313–3335. https://doi.org/10.1039/C1CS15042A

[14] Li, X.-B., Ma, Y., & Gao, E.-Q. (2018). Random Co(II)–Ni(II) ferromagnetic chains showing coexistent anti-ferromagnetism, metamagnetism, and single-chain magnetism. *Inorg. Chem*., 57, 7446–7454. https://doi.org/10.1021/acs.inorgchem.8b01053

[15] Wöhlert, S., Boeckmann, J., Wriedt, M., & Näther, C. (2011). Coexistence of metamagnetism and slow relaxation of the magnetization in a cobalt thiocyanate 2D coordination network. *Angew. Chem. Int. Ed.*, 50, 6920–6923. https://doi.org/10.1002/anie.201007899

[16] Li, Z.-X., Zhao, J.-P., Sanudo, E., Ma, H., Pan, Z.-D., Zeng, Y.-F., & Bu, X.-H. (2009). New 3D coordination polymers constructed from pillared metal− formate kagomé layers exhibiting spin canting only in the nickel (II) complex. *Inorg. Chem.*, 48, 11601–11607. https://doi.org/10.1021/ic901564y

[17] Li, G., Akitsu, T., Sato, O., & Einaga, Y. (2004). Synthesis, crystal structures and magnetic properties of two new hetero-bimetallic assemblies. *J. Coord. Chem*., 57, 189–198. https://doi.org/10.1080/00958970410001671093

[18] Willett, R. D., Gatteschi, D., & Kahn, O. (1985). Magneto-structural correlations in exchange coupled systems. D. Reidel Publishing Company. ISBN:9027718768 https://catalogue.nla.gov.au/catalog/1433851

[19] Li, Y.-H., He, W.-R., Ding, X.-H., Wang, S., Cui, L.-F., & Huang, W. (2012). Cyanide-bridged assemblies constructed from capped tetracyanometalate building blocks [MA (ligand)(CN) 4] 1−/2−(MA= Fe or Cr). *Coord. Chem. Rev.*, 256, 2795–2815. https://doi.org/10.1016/j.ccr.2012.09.014

[20] Zhang, D., Zhuo, S., Wang, P., Chen, X., & Jiang, J. (2014). A new series of cyanide-bridged heterobimetallic Fe III–Fe III/Mn III/Cu II one-dimensional complexes: Synthesis, crystal structures, and magnetic properties. *New J. Chem.*, 38, 5470–5479. https://doi.org/10.1039/C4NJ00743C

[21] Zhang, H., Xue, C., Shi, J., Liu, H., Dong, Y., Zhao, Z., & Jiang, J. (2016). Coordination field tuned cyanide-bridged polynuclear and one-dimensional heterobimetallic complexes: Synthesis, crystal structures, and magnetic properties. *Cryst. Growth Des.*, 16, 5753–5761. https://doi.org/10.1021/acs.cgd.6b00820

[22] Lan, W., Hao, X., Dou, Y., Zhou, Z., Yang, L., Liu, H., & Zhang, D. (2019). Various structural types of cyanide-bridged FeIII–MnIII bimetallic coordination polymers (CPs) and polynuclear clusters based-on a new mertricyanoiron (III) building block: Synthesis, crystal structures, and magnetic properties. *Polymers*, 11, 1585. https://doi.org/10.3390/polym11101585

[23] Wang, C.-F., Zuo, J.-L., Bartlett, B. M., Song, Y., Long, J. R., & You, X.-Z. (2006). Symmetry-based magnetic anisotropy in the trigonal bipyramidal cluster [Tp2 (Me3tacn) 3Cu3Fe2 (CN) 6] 4+. *J. Am. Chem. Soc.*, 128, 7162–7163. https://doi.org/10.1021/ja061788+

[24] Shao, D., Zhou, Y., Pi, Q., Shen, F.-X., Yang, S.-R., Zhang, S.-L., & Wang, X.-Y. (2017). Two-dimensional frameworks formed by pentagonal bipyramidal cobalt(II) ions and hexacyanometallates: antiferro-magnetic ordering, metamagnetism and slow magnetic relaxation. *Dalton Trans.*, 46, 9088–9096. https://doi.org/10.1039/C7DT01893B

[25] Gatteschi, D., & Sessoli, R. (2001). Single-molecule magnets: a new class of magnetic materials. *J. Alloys Compd*., 317–318, 180–182. https://doi.org/10.1016/S0925-8388(00)01407-9

[26] Schenker, R., Leuenberger, M. N., Chaboussant, G., Loss, D., & Güdel, H. U. (2005). Butterfly hysteresis and slow relaxation of the magnetization in (Et4N)3Fe2F9: manifestations of a single-molecule magnet. *Phys. Rev. B*, 72, 184403. https://doi.org/10.1016/S0009-2614(02)00670-X

[27] Zhang, L., Zhang, Y.-Q., Zhang, P., Gao, L., Ganguly, S., Shen, J., & Gao, S. (2020). Development of single-molecule magnets. *Chin. J. Chem*., 38, 1005–1018. https://doi.org/10.1002/cjoc.202000090

[28] Chilton, N. F. (2015). Design criteria for high-temperature single-molecule magnets. *Inorg. Chem*., 54, 2097–2099. https://doi.org/10.1021/acs.inorgchem.5b00089

[29] Moreno-Pineda, E., Damjanović, M., Ould-Moussa, N., Wernsdorfer, W., & Ruben, M. (2019). Quantum tunnelling of the magnetisation in single-molecule magnet isotopologue dimers. *Chem. Sci.*, 10, 5138–5145. https://doi.org/10.1039/C9SC01062A

[30] Zabala-Lekuona, A., Seco, J. M., & Colacio, E. (2021). Single-molecule magnets: From Mn12-ac to dysprosium metallocenes, a travel in time. Coord. *Chem. Rev.*, 441, 213984. https://doi.org/10.1016/j.ccr.2021.213984

[31] Wu, W., Huang, T., Zhu, J., Zou, T., & Wang, H. (2025). Exploring single-molecular magnets for quantum technologies. *Molecules*, 30, 2522. https://doi.org/10.3390/molecules30122522

[32] Zhang, X., Li, X., & Yang, J. (2019). Molecular spintronics. *J. Appl. Phys.*, 125, 240401. https://doi.org/10.1063/1.5113900

[33] Frost, J. M., Harriman, K. L. M., & Murugesu, M. (2016). The rise of 3d single-ion magnets in molecular magnetism: towards materials from molecules? *Chem. Sci.*, 7, 2470–2491. https://doi.org/10.1039/C5SC03224E

[34] Pedersen, K. S., Bendix, J., & Clérac, R. (2014). Single-molecule magnet engineering: building-block strategies for high-temperature molecular nanomagnets. *Chem. Commun.*, 50, 4396–4415. https://doi.org/10.1039/C4CC00339J

[35] Woodruff, D. N., Winpenny, R. E. P., & Layfield, R. A. (2013). Lanthanide single-molecule magnets. *Chem. Rev.*, 113, 5110–5148. https://doi.org/10.1021/cr400018q

[36] Majcher, A. M., Pilet, G., Mironov, V. S., & Vostrikova, K. E. (2017). Neutral low-dimensional assemblies of a Mn(III) Schiff base complex and octacyanotungstate(V): Synthesis, characterization, and magnetic properties. *Magnetochemistry*, 3, 16. https://doi.org/10.3390/magnetochemistry3020016

[37] Qian, K., Huang, C.-X., Zhou, C., You, Z.-Z., Wang, X.-Y., & Hunber, K. R. (2013). A single-molecule magnet based on heptacyanomolybdate with the highest energy barrier for a cyanide compound. *J. Am. Chem. Soc.*, 135, 13302–1330. https://doi.org/10.1021/ja4067833

[38] Mrozek, J., Szklarzewicz, J., & Nitek, W. (2015). Magnetic clusters based on octacyanidometallates. *Inorg. Chem. Front.*, 2, 184–192. https://doi.org/10.1039/C4QI00189C

[39] Marvaud, V. (2002). Structural diversity of cyanide-bridged bimetallic clusters based on hexacyanometallate building blocks. *C. R. Chim*., 5, 289–295. https://doi.org/10.1016/S1631-0748(02)01429-7

[40] Atanasov, M., Comba, P., & Daul, C. A. (2006). DFT studies on the magnetic exchange across the cyanide bridge. *J. Phys. Chem. A*, 110, 13332–13340. https://doi.org/10.1021/jp066020q

[41] Liu, K., Zhang, X., Meng, X., Shi, W., Cheng, P., & Powell, A. K. (2016). Constraining the coordination geometries of lanthanide centers and magnetic building blocks in frameworks: a new strategy for molecular nanomagnets. *Chem. Soc. Rev.,* 45, 2423–2439. https://doi.org/10.1039/C5CS00770D

[42] Yao, X.-N., Du, J.-Z., Zhang, Y.-Q., Leng, X.-B., Yang, M.-W., Lin, S.-D., Shao, Z.-X., An, Z., & Kong, L. (2017). Two-coordinate Co(II) imido complexes as outstanding single-molecule magnets. *J. Am. Chem. Soc.*, 139, 373–380. https://doi.org/10.1021/jacs.6b11043

[43] Zhang, S., Tang, J., Zhang, J., Xu, F., Chen, S., Hu, D., & Yin, B. (2019). Designing a mononuclear DyIII single-molecule magnet (SMM) by using a N,O,N,O-based multichelating Schiff base ligand and a β-diketonate ligand. *New J. Chem.,* 43, 454–462. https://doi.org/10.1039/C8NJ04019B

[44] Xin, Y., Wang, B., Autschbach, J., Zaykov, A., Nikitin, E. V., Vlasov, M. Y., Fedin, M. V., Ovchorenko, V. I., & Pinkowicz, D. (2023). Desolvation-induced highly symmetrical terbium(III) sin-gle-molecule magnet exhibiting luminescent self-monitoring of temperature. *Angew. Chem. Int. Ed.*, 62, e202306372. https://doi.org/10.1002/ange.202306372

[45] Maniaki, D., Pilichos, E., & Perlepes, S. P. (2018). Coordination clusters of 3d-metals that behave as single-molecule magnets (SMMs): Synthetic routes and strategies. *Front. Chem.*, 6, 461. https://doi.org/10.3389/fchem.2018.00461

[46] Rosado Piquer, L., & Sañudo, E. C. (2015). Heterometallic 3d–4f single-molecule magnets. *Dalton Trans.*, 44, 8771–8780. https://doi.org/10.1039/C5DT00549C

[47] Endicott, J. F., & Chen, Y.-J. (2013). Electronic coupling between metal ions in cyanide-bridged ground state and excited state mixed valence complexes*. Coord. Chem. Rev.*, 257, 1676–1698. https://doi.org/10.1016/j.ccr.2012.10.018

[48] Shatruk, M., Avendano, C., & Dunbar, K. R. (2009). Cyanide-bridged complexes of transition metals: A molecular magnetism perspective. *Prog. Inorg. Chem.*, 56, 155–334. https://doi.org/10.1002/9780470440124.ch3

[49] Qi, M., Dong, Q., Wang, D., & Byers, J. A. (2018). Electrochemically switchable ring-opening polymerization of lactide and cyclohexene oxide. *J. Am. Chem. Soc.,* 140, 5686–5690. https://doi.org/10.1021/jacs.8b02171

[50] Abbasi, P., Quinn, K., Alexandropoulos, D. I., Damjanovic, M., Wernsdorfer, W., Escuer, A., & Sta-matatos, T. C. (2017). Transition metal single-molecule magnets: a {Mn31} nanosized cluster with a large energy barrier of ∼ 60 K and magnetic hysteresis at ∼ 5 K. *J. Am. Chem. Soc.,* 139, 15644–15647. https://doi.org/10.1021/jacs.7b10130

[51] Zhang, H., Mao, Z., Kang, Y., Zhang, W., Mei, L., & Ji, X. (2023). Redox regulation and its emerging roles in cancer treatment. Coord. *Chem. Rev.,* 475, 214897. https://doi.org/10.1016/j.ccr.2022.214897

[52] Ortiz, J. H. M., Longo, C., & Katz, N. E. (2015). Polypyridyl ruthenium complexes containing anchoring nitrile groups as TiO2 sensitizers for application in solar cells. *Inorg. Chem. Commun.*, 55, 69–72. https://doi.org/10.1016/j.inoche.2015.03.009

[53] Shoaib, M., Vallayil, P., Jaiswal, N., Iyapazham Vaigunda Suba, P., Sankararaman, S., Ramanujam, K., & Thangadurai, V. (2024). Advances in redox flow batteries–A comprehensive review on inorganic and organic electrolytes and engineering perspectives. *Adv. Energy Mater.*, 14, 2400721. https://doi.org/10.1002/aenm.202400721

[54] Li, M.-H., You, M.-H., & Lin, M.-J. (2021). Photochromism and photomagnetism in three cyano-bridged 3d–4f heterobimetallic viologen frameworks. *Dalton Trans.*, 50, 4959–4966. https://doi.org/10.1039/D0DT04358C

[55] Mercurol, J., Li, Y., Pardo, E., Risset, O., Seuleiman, M., Rousseliere, H., & Julve, M. (2010). [FeIILSCoIIILS] 2 ⇔ [FeIIILSCoIIHS] 2 photoinduced conversion in a cyanide-bridged heterobimetallic molecular square. *Chem. Commun.*, 46, 8995–8997. https://doi.org/10.1039/C0CC02024A

[56] Chow, C.-F., Chiu, B. K., Lam, M. H., & Wong, W.-Y. (2003). A trinuclear heterobimetallic Ru(II)/Pt(II) complex as a chemodosimeter selective for sulfhydryl-containing amino acids and peptides. *J. Am. Chem. Soc.*, 125, 7802–7803. https://doi.org/10.1021/ja034891x

[57] Kisel, K. S., Melnikov, A. S., Grachova, E. V., Karttunen, A. J., Doménech-Carbó, A., Monakhov, K. Y., & Koshevoy, I. O. (2019). Supramolecular construction of cyanide-bridged ReI diimine multichromophores. *Inorg. Chem.*, 58, 1988–2000. https://doi.org/10.1021/acs.inorgchem.8b02974

[58] Ibrahim, S., Cheng, Y., Zhao, D., & Nadeem, M. A. (2019). A new insight for photocatalytic hydrogen production by a Cu/Ni based cyanide bridged polymer as a co-catalyst on titania support in glycerol water mixture*. Int. J. Hydrogen Energy*, 44, 2508–2518. https://doi.org/10.1016/j.ijhydene.2018.12.045

[59] Zhu, X.-Q., & Sheng, T.-L. (2020). Syntheses, crystal structures and magnetic properties of redox active cyanide-bridged trinuclear Ru-M2 (M= Co, Ni, Cu) complexes. *Inorg. Chem. Commun.,* 111, 107638. https://doi.org/10.1016/j.inoche.2019.107638

[60] Sun, L., Belmouri, N. E. I., Ndiaye, M., Robeyns, K., Rotaru, A., Boukheddaden, K., & Garcia, Y. (2023). Thermal-driven guest-induced spin crossover behavior in 3D Fe(II)-based porous coordination polymers. *Cryst. Growth Des.*, 23, 3402–3411. https://doi.org/10.1021/acs.cgd.2c01538

[61] Guo, M. (2017). *Electronic structure investigations of transition metal complexes through X-ray spectroscopy* [Ph.D. Thesis, Uppsala University]. ISBN:978-91-513-0035-1 https://uu.diva-portal.org/smash/record.jsf?pid=diva2%3A1133777&dswid=1738

[62] Tsaturyan, A. A., Budnyk, A. P., & Ramalingan, C. (2019). DFT study of the CNS ligand effect on the geometry, spin-state, and absorption spectrum in ruthenium, iron, and cobalt quaterpyridine complex-es. *ACS Omega*, 4, 10991–11003. https://doi.org/10.1021/acsomega.9b00921

[63] Getzner, L., Paliwoda, D., Vendier, L., Lawson-Daku, L. M., Rotaru, A., Molnár, G., Cobo, S., & Bousseksou, A. (2024). Combining electron transfer, spin crossover, and redox properties in metal-organic frameworks. *Nat. Commun.*, 15, 7192. https://doi.org/10.1038/s41467-024-51385-8

[64] Nandy, A., Duan, C., Taylor, M. G., Liu, F., Steeves, A. H., & Kulik, H. J. (2021). Computational discovery of transition-metal complexes: From high-throughput screening to machine learning. *Chem. Rev.*, 121, 9927–10000. https://doi.org/10.1021/acs.chemrev.1c00347

[65] Toney, J. W., St. Michel, R. G., Garrison, A. G., Kevlishvili, I., & Kulik, H. J. (2025). Graph neural networks for predicting metal-ligand coordination of transition metal complexes. *Proc. Natl. Acad. Sci. U.S.A.*, 122, e2415658122. https://doi.org/10.1073/pnas.2415658122

[66] Xie, Y., Lin, R.-B., & Chen, B. (2022). Old materials for new functions: Recent progress on metal cyanide based porous materials. *Adv. Sci.*, 9, 2104234. https://doi.org/10.1002/advs.202104234

[67] Lord, R. L., & Baik, M.-H. (2008). Why does cyanide pretend to be a weak field ligand in [Cr(CN)5]3–? *In-org. Chem.*, 47, 4413–4420. https://doi.org/10.1021/ic8000653

[68] Li, J., Lord, R. L., Noll, B. C., Baik, M.-H., Schulz, C. E., & Scheidt, W. R. (2008). Cyanide—a strong field ligand for ferrohemes and hemoproteins? *Angew. Chem. Int. Ed.*, 47, 10144–10146. https://doi.org/10.1002/anie.200804116

[69] Singh, S. K., & Rajaraman, G. (2016). Deciphering the origin of giant magnetic anisotropy and fast quantum tunnelling in rhenium(IV) single-molecule magnets. *Nat. Commun.*, 7, 10669. https://doi.org/10.1038/ncomms10669

[70] Gupta, T., & Rajaraman, G. (2018). Magnetic anisotropy, magneto-structural correlations and mechanism of magnetic relaxation in DyIIIN8 complexes: A theoretical perspective. *Eur. J. Inorg. Chem.*, 2018, 3402–3412. https://doi.org/10.1002/ejic.201800350

[71] Cornia, A., Barra, A.-L., Bulicanu, V., Clérac, R., Cortijo, M., Hillard, E. A., Galavotti, R., Lunghi, A., Nicolini, A., Rouzières, M., Sorace, L., & Totti, F. (2020). The origin of magnetic anisotropy and single-molecule magnet behavior in chromium(II)-based extended metal atom chains. *Inorg. Chem*., 59, 1763–1777. https://doi.org/10.1021/acs.inorgchem.9b02994

[72] Deeth, R. J. (2024). Ligand field theory, Pauli shields and ultra-covalency in organometallic chemistry. *Phys. Chem*., 26, 18138–18148. https://doi.org/10.1039/D4CP00764F

[73] Cohen, A. J., Mori-Sánchez, P., & Yang, W. (2012). Challenges for density functional theory. *Chem. Rev.*, 112, 289–320. https://doi.org/10.1021/cr200107z

[74] Atanasov, M., Daul, C. A., & Rauzy, C. (2004). Ground states, excited states, and metal–ligand bonding in rare earth hexachloro complexes: A DFT based ligand field theory. *Struct. Bond.*, 106, 97–125. https://doi.org/10.1007/b11340

[75] Illas, F., de P. R. Moreira, I., Bofill, J. M., & Filatov, M. (2004). Extent and limitations of density-functional theory in describing magnetic systems. *Phys. Rev. B*, 70, 132414. https://doi.org/10.1103/PhysRevB.70.132414

[76] Cirera, J., & Ruiz, E. (2017). Modeling magnetic properties with density functional theory-based methods. In B. Sieklucka & D. Pinkowicz (Eds.), Molecular magnetic materials: Concepts and applications (pp. 419–447). Wiley-VCH Verlag GmbH & Co. KGaA. https://doi.org/10.1002/9783527694228.ch17

[77] Fitzhugh, H. C., Furness, J. W., Pederson, M. R., Peralta, J. E., & Sun, J. (2023). Comparative density functional theory study of magnetic exchange couplings in dinuclear transition-metal complexes. *J. Chem. Theory Comput*., 19, 5760–5772. https://doi.org/10.1021/acs.jctc.3c00336

[78] Sugisaki, K., Toyota, K., Sato, K., Shiomi, D., & Takui, T. (2017). Behavior of DFT-based approaches to the spin-orbit term of zero-field splitting tensors: a case study of metallocomplexes, M(acac)3 (M = V, Cr, Mn, Fe and Mo). *Phys. Chem. Chem. Phys.*, 19, 30128–30138. https://doi.org/10.1039/C7CP05533A

[79] Atanasov, M., Comba, P., & Daul, C. A. (2008). Combined ligand field and density functional theory analysis of the magnetic anisotropy in oligonuclear complexes based on exchange-coupled pairs. *In-org. Chem.,* 47, 2449–2463. https://doi.org/10.1021/ic701702x

[80] Maschietto, F., Campetella, M., Sanz García, J., Adamo, C., & Ciofini, I. (2021). Chasing unphysical TD-DFT excited states in transition metal complexes with a simple diagnostic tool*. J. Chem. Phys.,* 154, 204102. https://doi.org/10.1063/5.0050680

[81] Rahbani, N., de Silva, P., & Baudrin, E. (2023). Density functional theory-based protocol to calculate the redox potentials of first-row transition metal complexes for aqueous redox targeting flow batteries. *ChemSusChem*, 16, e202300482. https://doi.org/10.1002/cssc.202300482

[82] Lancaster, K. M., Gerken, J. B., Durrell, A. C., Palmer, J. H., & Gray, H. B. (2010). Electronic structures, photophysical properties, and electrochemistry of ruthenium(II) (bpy)2 pyridylimidazole complexes. *Coord. Chem. Rev.*, 254, 1803–1811. https://doi.org/10.1016/j.ccr.2010.04.005

[83] Jankowski, R., Wyczesany, M., & Chorazy, S. (2023). Multifunctionality of luminescent molecular nanomagnets based on lanthanide complexes. *Chem. Commun.*, 59, 5961–5986. https://doi.org/10.1039/D3CC00342F

[84] Sessoli, R., Gatteschi, D., Caneschi, A., & Novak, M. A. (1993). Magnetic bistability in a metal-ion cluster. *Nature*, 365, 141–143. https://www.nature.com/articles/365141a0

[85] Wernsdorfer, W., & Sessoli, R. (1999). Quantum phase interference and parity effects in magnetic molecular clusters. *Science*, 248, 133–135. https://www.science.org/doi/10.1126/science.284.5411.133

[86] Gatteschi, D., & Sessoli, R. (2003). Quantum tunneling of magnetization and related phenomena in molecular materials. *Angew. Chem. Int. Ed.*, 42, 268–297. https://onlinelibrary.wiley.com/doi/10.1002/anie.200390099

[87] Mannini, M., Pineider, F., Sainctavit, P., Danieli, C., Otero, E., Sciancalepore, C., Talarico, A. M., Arrio, M.-A., Cornia, A., Gatteschi, D., & Sessoli, R. (2009). Magnetic memory of a single-molecule quantum magnet wired to a gold surface. *Nat. Mater.*, 8, 194–197. https://www.nature.com/articles/nmat2374

[88] Mannini, M., Pineider, F., Danieli, C., Totti, F., Sorace, L., Sainctavit, P., Arrio, M. A., Otero, E., Joly, L., Cezar, J. C., Cornia, A., & Sessoli, R. (2010). Quantum tunnelling of the magnetization in a monolayer of oriented single-molecule magnets. *Nature,* 468, 417. https://www.nature.com/articles/nature09478

[89] Leuenberger, M. N., & Loss, D. (2001). Quantum computing in molecular magnets. *Nature,* 410, 789–793. https://www.nature.com/articles/35071024

[90] Hill, S., Edwards, R. S., Aliaga-Alcalde, N., & Christou, G. (2003). Quantum coherence in an ex-change-coupled dimer of single-molecule magnets. *Science*, 302, 1015–1018. https://www.science.org/doi/10.1126/science.1090082

[91] Plass, W., Pohlmann. A., & Rautengarten, J. (2001). Magnetic interactions as supramolecular function: Structure and magnetic properties of hydrogen-bridged dinuclear copper(II) complexes. *Angew. Chem. Int. Ed.*, 40, 4207–4210.

[92] Desplanches, C., Ruiz, E., Rodrı´guez-Fortea, A., & Alvarez, S. (2002). Exchange coupling of transition-metal ions through hydrogen bonding: A theoretical investigation*. J. Am. Chem. Soc.*, 124, 5197–5205. https://doi.org/10.1021/ja0178160

[93] Costa, J. S. N., Bandeira, N. A. G., Le Guennic, B., Robert, V., Gamez, P., Chastanet, G., Ortiz-Frade, L., & Gasque, L. (2011). Coexistence of Intramolecular Ligand-Mediated and Through Hydrogen-Bond Magnetic Interactions in a Chain of Dicopper(II) Units. *Inorg. Chem.*, 50, 5696–5705. https://pubs.acs.org/doi/10.1021/ic200480d

[94] Schmidt, J. A., Johnson, M. S., Grage, M. M. L., & Nyman, G. (2009). On the origin of the asymmetric shape of the HCl photodissociation cross section. *Chemical Physics Letters*, *480*(4-6), 168-172. https://doi.org/10.1016/j.cplett.2009.09.014

[95] Tupolova, Y. P., Lebedev, V. E., Lazarenko, V. A., Shcherbakov, I. N., Levchenkov, S. I., Popov, L. D., Minin, V. V., Efimov, N. N., Zubavichus, Y. V., & Zubenko, A. A. (2021). Unprecedented interplay of antiferro- and ferromagnetic exchange interactions through intermolecular hydrogen bonds in mononuclear Cu(II) complexes. *New J. Chem.*, 45, 12236–12246. https://doi.org/10.1039/D1NJ01440D

[96] Griffith, J. S. (1964). The theory of transition metal ions. Cambridge University Press.

[97] Abragam, A., & Bleaney, B. (1970). Electron paramagnetic resonance of transition ions. Clarendon Press.

[98] Solomon, E. I., & Lowery, M. D. (1993). Electronic structure contributions to function in bioinorganic chemistry. *Science*, 259, 1575. https://www.science.org/doi/10.1126/science.8384374

[99] Neese, F., & Solomon, E. I. (1998). Calculation of zero-field splittings, g-values, and the relativistic nephelauxetic effect in transition metal complexes. Application to high-spin ferric complexes*. Inorg. Chem.*, 37, 6568–6582. https://pubs.acs.org/doi/10.1021/ic980948i

[100] Luo, Q.-C., & Zheng, Y.-Z. (2021). Methods and models of theoretical calculation for single-molecule magnets. *Magnetochemistry*, 7, 107. https://www.mdpi.com/2312-7481/7/8/107

[101] Pryce, M. H. L. (1950). A modified perturbation procedure for a problem in paramagnetism. *Proc. Phys. Soc*. (London), A63, 25. https://iopscience.iop.org/article/10.1088/0370-1298/63/1/304

[102] Abragam, A., & Pryce, M. H. L. (1951). Theory of the nuclear hyperfine structure of paramagnetic resonance spectra in crystals. *Proc. R. Soc.*, A205, 135. https://royalsocietypublishing.org/rspa/article/205/1080/135/8402/Theory-of-the-nuclear-hyperfine-structure-of

[103] Chiesa, A., Cugini, F., Hussain, R., Macaluso, E., Allodi, G., Garlatti, E., Giansiracusa, M., Goodwin, C. A. P., Ortu, F., Reta, D., et al. (2020). Understanding magnetic relaxation in single-ion magnets with high blocking temperature. *Phys. Rev. B*, 101, 174402. https://journals.aps.org/prb/abstract/10.1103/PhysRevB.101.174402